Science of the Total Environment 693 (2019) 133491

Contents lists available at ScienceDirect

Science of the Total Environment

journal homepage: www.elsevier.com/locate/scitotenv

Potential effects of deep seawater discharge by an Ocean Thermal Energy Conversion plant on the marine microorganisms in oligotrophic waters

Mélanie Giraud [a,b,c], Véronique Garçon [b], Denis de la Broise [a], Stéphane L'Helguen [a], Joël Sudre [b], Marie Boye [a,d,*]

[a] LEMAR (UMR 6539), IUEM, Technopôle Brest-Iroise, 29280 Plouzané, France
[b] LEGOS (UMR 5566), 31401 Toulouse cedex 9, France
[c] France Energies Marines, 29200 Brest, France
[d] Institut de Physique du Globe de Paris (UMR 7154), 75005 Paris, France

HIGHLIGHTS

- Cold deep seawater discharge generated by an OTEC plant has negligible thermic impact on the phytoplankton assemblage
- Discharge of 10% deep seawater at chlorophyll-*a* maximum depth induces large shift in the phytoplankton community structure.
- Microbial effect was limited with 2% deep water addition and negligible with discharge at the bottom of euphotic layer depth
- First environmental standards for discharge depth to exploit OTEC plant without harmful effects on the microbial community

GRAPHICAL ABSTRACT

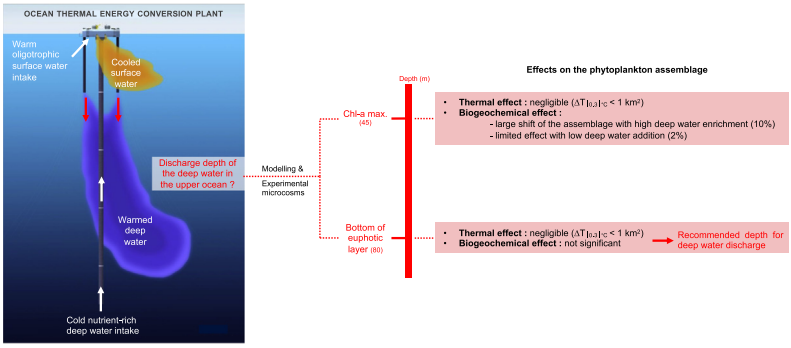

ARTICLE INFO

Article history:
Received 21 February 2019
Received in revised form 2 July 2019
Accepted 18 July 2019
Available online 19 July 2019

Editor: Julian Blasco

Keywords:
Marine microbial ecosystem
Biogeochemistry
Modeling
Artificial seawater discharge
in situ experiments
Environmental standards

ABSTRACT

Installation of an Ocean Thermal Energy Conversion pilot plant (OTEC) off the Caribbean coast of Martinique is expected to use approximately 100,000 $m^3\ h^{-1}$ of deep seawater for its functioning. This study examined the potential effects of the cold nutrient-rich deep seawater discharge on the phytoplankton community living in the surface warm oligotrophic waters before the installation of the pilot plant. Numerical simulations of deep seawater upwelled by the OTEC, showed that a 3.0 °C temperature change, considered as a critical threshold for temperature impact, was never reached during an annual cycle on the top 150 m of the water column on two considered sections centered on the OTEC. The thermal effect should be limited, <1 km^2 on the area exhibited a temperature difference of 0.3 °C (absolute value), producing a negligible thermic impact on the phytoplankton assemblage. The impact on phytoplankton of the resulting mixed deep and surface seawater was evaluated by *in situ* microcosm experiments. Two scenarios of water mix ratio (2% and 10% of deep water) were tested at two incubation depths (deep chlorophyll-*a* maximum: DCM and bottom of the euphotic layer: BEL). The larger impact was obtained at DCM for the highest deep seawater addition (10%), with a development of diatoms and haptophytes, whereas 2% addition induced only a limited change of the phytoplankton community (relatively higher *Prochlorococcus* sp. abundance, but without significant shift of the assemblage). This study suggested that the OTEC plant would significantly modify the phytoplankton assemblage with a shift from pico-phytoplankton toward micro-phytoplankton only in the case of a discharge affecting the DCM and would be

* Corresponding author at: Institut de Physique du Globe de Paris (UMR 7154), France.
E-mail address: boye@ipgp.fr (M. Boye).

https://doi.org/10.1016/j.scitotenv.2019.07.297

restricted to a local scale. Since the lower impact on the phytoplankton assemblage was obtained at BEL, this depth can be recommended for the discharge of the deep seawater to exploit the OTEC plant.

1. Introduction

Ocean Thermal Energy Conversion (OTEC) uses the solar energy by exploiting the temperature gradient between surface and bottom seawater. In an OTEC plant, the cold deep seawater pumped close to sea bottom is used to condense a working fluid (like ammonia), whereas warm surface waters, pumped close to the surface, serve to evaporate it. The difference of pressure, generated by the evaporation and condensation of the fluid, drives a turbine that produces mechanical energy. This energy is then converted to electrical energy in a generator. Due to the need of a 20 °C difference between the cold deep and the warm surface waters for the OTEC exploitation, tropical areas are well suited for the installation of OTEC plants.

The Martinique, a tropical island of Lesser Antilles, is ideally suited for OTEC functioning with its narrow continental slope in the Caribbean part of the island, allowing an implementation of the plant close to the coast. The implementation of a 10 MW OTEC pilot plant off the Caribbean coast of Martinique is expected in 2020 as part of the French NEMO project (Akuo Energy, DCNS). This OTEC will pump approximately 100,000 $m^3.h^{-1}$ of deep seawater at 1100 m depth. In order to optimize the energy efficiency, the deep seawater should be rejected close to the surface. However, this large discharge could induce important disturbances on the upper ocean ecosystem, and this impact should be estimated.

Environmental assessment of OTEC functioning was studied since the 1980's (NOAA, 1981, 2010). The deep seawater discharge was described as one of the major drivers impacting the marine environment in OTEC plant. However, only a few studies specifically detailed this critical aspect (Taguchi et al., 1987; Rocheleau et al., 2012). The deep seawater discharge in OTEC plant generates a phenomenon similar to the one naturally occurring in the ocean within upwelling systems. Equatorward winds along the coast in the eastern Atlantic and Pacific linked to atmospheric high-pressure systems force Ekman transport and pumping, relocating coastal surface waters offshore. Thereby, deep water transport toward the surface is generated close to the coast. In these systems, the large amount of macronutrients and trace metals carried to the euphotic zone by the enriched deep seawater supports a large development of the phytoplankton, making upwelling the most productive oceanic regions (Bakun, 1990; Pauly and Christensen, 1995; Chavez and Toggweiler, 1995; Carr and Kearns, 2003). By contrast, the tropical surface waters off the Caribbean coast of Martinique exhibit low nutrients (nitrate and phosphate) concentrations (<0.02 $\mu mol.L^{-1}$) and therefore, they can be significantly enriched by the deep seawater discharge. Whereas phytoplankton assemblages in upwelling systems are usually dominated by large phytoplankton and particularly by diatoms (Bruland et al., 2001; Van Oostende et al., 2015), the phytoplankton community in oligotrophic systems is composed of smaller organisms (Agawin et al., 2000).

Due to these important differences in biogeochemical functioning and environmental microbiology, it is thus of critical interest to investigate the potential effects of the deep seawater discharge of the planned OTEC plant on the phytoplankton community off Martinique. Furthermore, it is crucial to provide a depth where the deep seawater could be discharged without significant effect on the surface layer where phytoplankton is the most abundant. Indeed, no environmental standards on the deep seawater discharge effects are available yet, while transitional blue energies such as OTEC plants will likely expand in the near future.

In this study, the impact of deep seawater discharge on the thermal structure of surface waters was first assessed. Modification of the surface waters stratification should indeed impact the phytoplankton community. A high-resolution oceanic model was used to examine the thermal impact induced by the deep seawater dispersion. Eight configurations of discharge depth were tested, corresponding to the deep chlorophyll-*a* maximum (DCM), the bottom of the euphotic layer (BEL) and five depths below the BEL. Temperature differences between numerical simulations without and with the deep seawater discharge were compared on the upper 150 m of a vertical section.

The distribution of the ambient phytoplankton community and the biogeochemical properties of the deep and surface seawater mixture that could impact the phytoplankton community were then described. Phytoplankton distribution and assemblage were detailed in order to assess short time and small scales variabilities of phytoplankton assemblage and primary production in the study site.

Finally, in order to simulate the OTEC deep seawater input, enrichment experiments were conducted on the future site of the pilot plant. Enrichment experiments are commonly used in oceanography to assess the effects on phytoplankton community and primary production. For example, large iron (Fe) enrichment experiments were conducted from 1993 to 2005 to estimate the potential of Fe limitation on ocean primary production (De Baar et al., 2005; Boyd et al., 2007). Several experiments also showed that macro- and micro-nutrients enrichments induce changes in the phytoplankton community in upwelling regions (Hutchins et al., 2002) as well as in oligotrophic regions (Kress et al., 2005). Enrichment experiments were usually conducted with mesocosms immerged close to the surface (Escaravage et al., 1996; Duarte et al., 2000) or in laboratory under artificial light and temperature using phytoplankton model species (Brzezinski, 1985). A laboratory experiment intended to evaluate the effects of an OTEC seawater discharge in Hawaiian waters on the natural phytoplankton community was previously conducted (Taguchi et al., 1987) under such artificial conditions, and thus, it could not totally reproduce what occurred in the natural environment. Other deep seawater discharge experiments were realized *in situ* (Aure et al., 2007; Handå et al., 2014). For example, the use of a moored platform to upwell deep seawater and discharge it close to the surface has shown an increase in primary production in a western Norwegian fjord where the euphotic zone is nutrient-depleted during summer (Aure et al., 2007), as it would be expected with the OTEC discharge in oligotrophic waters. Whereas such a pumping system is well adapted for pumping seawater at 30 m depth for example, it cannot be applied for OTEC experiments where deep seawater must be collected far deeper (1100 m depth) and also discharged more deeply in the water column to reduce the potential effects on the phytoplankton community. These conditions can be obtained by the use of *in situ* microcosms, in which light and temperature are the same as in the natural surrounding waters, avoiding additional bias, and several conditions (enrichment, incubation depth) can be simulated. Therefore, we used the unique device of immerged microcosms we developed (Giraud et al., 2016) for assessing the effects of deep seawater discharge on the phytoplankton community. Two incubation depths (DCM and BEL) with two ratios of enriched seawater (mixtures of surface water with 2% and 10% of deep seawater) were tested.

These experiments allowed the evaluation of critical mixing rate and discharging depth where effect was maximal.

2. Materials and methods

2.1. Modelling the thermal effect

The hydrodynamic numerical model ROMS-Regional Ocean Model System (Shchepetkin and McWilliams, 2005, 2009) was used to

describe the resulting thermal effect due to OTEC functioning. The model was run in a 2-ways AGRIF configuration allowing to define a parent and child domains around the Martinique Island which are run simultaneously, transferring automatically open boundary conditions. The parent grid ranges from 63° W to 59° W and 13° N to 15.9° N with a resolution of 1/60° (around 1.8 km) while the child domain narrows the parent one and was from 61.74° W to 60.41° W and 14.21° N to 15.11° N with a resolution down to 1/180° (around 600 m). The bottom topography and coastline are interpolated from the GINA database (1/120°, www.gina.alaska.edu/data/gtopo-dem-bathymetry) (Fig. 1). The model is forced by the monthly Climate Forecast System Reanalysis (NCEP-CFSR) for wind stress, heat and freshwater fluxes. For the open boundary conditions and initial conditions of the parent domain, a monthly climatology computed from the Simple Ocean Data Assimilation (SODA) reanalysis (Carton and Giese, 2008) was used for the dynamical variables (temperature, salinity and velocity fields). The configurations were run without and with a deep seawater discharge mimicking the OTEC functioning (Giraud, 2016). Eight cases of horizontal discharge settings were simulated at different depths: i) the DCM (45 m), ii) the BEL (80 m), that were estimated on June 12th 2014, and 3) six depths below the euphotic zone (110 m, 140 m, 170 m, 250 m, 350 m and 500 m). In the OTEC plant, deep water will be pumped at 1100 m where temperature is around 5 °C and salinity 35. Circulation of this water through the plant system will warm it up until 8 °C prior to its release in the upper ocean. We thus applied at the location of the OTEC plant (61°13′0″ W, 14°35′48″ N), a cold-water discharge (temperature 8 °C, salinity 35) at a flow rate of 28 $m^3\ s^{-1}$ and with a northward orientation. The thermal impact of the cold-water source was assessed documenting the differences between simulations without and with the modeled OTEC plant functioning (Giraud, 2016).

2.2. Field observations and in situ experiments

2.2.1. Sampling and analytical methods

Temperature, salinity, and fluorescence profiles were performed on 12th, 13th, 18th and 19th of June 2014 using Seabird SBE19+ probe with *in situ* Fluorimeter Chelsea AQUAtracka III.

Seawater was collected on 12th and 18th of June 2014 in the water column in ultra-clean conditions (Giraud et al., 2016) to measure *in situ* parameters and to prepare the microcosms. Seawater and microcosms were sampled similarly in a land laboratory a few hours after collection.

Nitrate (NO_3^-), nitrite (NO_2^-), phosphate (PO_4^{3-}) and silicate ($Si(OH)_4$) concentrations were determined in filtered waters (<0.6 μm; PC membrane) stored at −20 °C until analysis using a Bran + Luebbe AAIII auto-analyzer (Aminot et al., 2007).

Filtered samples (0.2 μm; 300 AC-Sartobran™ capsules) for dissolved trace metals determination were collected under pure-N_2 pressure (0.7 atm) in acid cleaned low density polyethylene bottles, acidified with ultrapure HCl (pH < 2) and stored in two plastic bags in dark at ambient temperature. Concentrations of dissolved trace metals (cadmium: Cd; lead: Pb; iron: Fe; zinc: Zn; manganese: Mn; cobalt: Co; nickel: Ni; and copper: Cu) were determined in UV-digested samples by ID-ICP-MS (Milne et al., 2010) after preconcentration on a WAKO resin (Kagaya et al., 2009) using an Element XR ICP-MS. Blanks, limits of detection, accuracy and precision (assessed using reference samples) of the ID-ICP-MS method are reported in Table 1. The values determined by ID-ICP-MS were in excellent agreement with the consensus values, apart for Cd that yielded higher concentration in S-SAFE reference sample than the consensus value (Table 1).

The pH was determined using a pH ultra-electrode (pHC28) mounted on a HQ40d multi pH-meter (HACH) with an accuracy of ± 0.002 pH unit in samples preserved with saturated $HgCl_2$ in glass bottles hermetically closed with Apiezon grease, sealed with Parafilm® and stored in the dark at ambient temperature.

Three complementary methods were used to analyze the phytoplankton community. Pigment signatures were measured by HPLC (using an Agilent Technologies 1100-series) on polysulfone filters (0.22 μm pore-size) frozen at −20 °C and stored in liquid nitrogen, after internal standard addition (vitamin E acetate) and extraction in a 100% methanol solution (Hooker et al., 2012). Fifty pigments were identified and associated to phytoplankton groups (Uitz et al., 2010). Identification and enumeration of pico-phytoplankton were realized by flow-cytometry using a BD-FACSVerse™ (Marie et al., 1999) in samples preserved in cryotube with addition of 0.25% glutaraldehyde frozen at −20 °C and stored in liquid nitrogen. Four groups of pico-phytoplankton were identified: *Prochlorococcus*, picoeukaryotes (<10 μm), and 2 groups of *Synechococcus* discriminated, respectively, by their low and high phycourobilin (PUB) to phycoerythrobilin (PEB) ratios. Taxonomic identification and enumeration of micro-phytoplankton (20–200 μm) and a part of nano-phytoplankton (2–20 μm) (Dussart, 1966) were carried out using an inverted microscope (Wild M40) in samples preserved with neutral lugol solution. Utermöhl settling chambers (Hasle, 1988) were used for micro-phytoplankton analyses, and a smaller sedimentation chamber (2.97 mL) for the analyses of nano-phytoplankton. When possible, phytoplankton was identified to the lowest possible taxonomic level (species, genus or group) using the classical manual for marine phytoplankton identification (Thomas, 1996) and the World Register of Marine Species database (WoRMS Editorial Board, 2019).

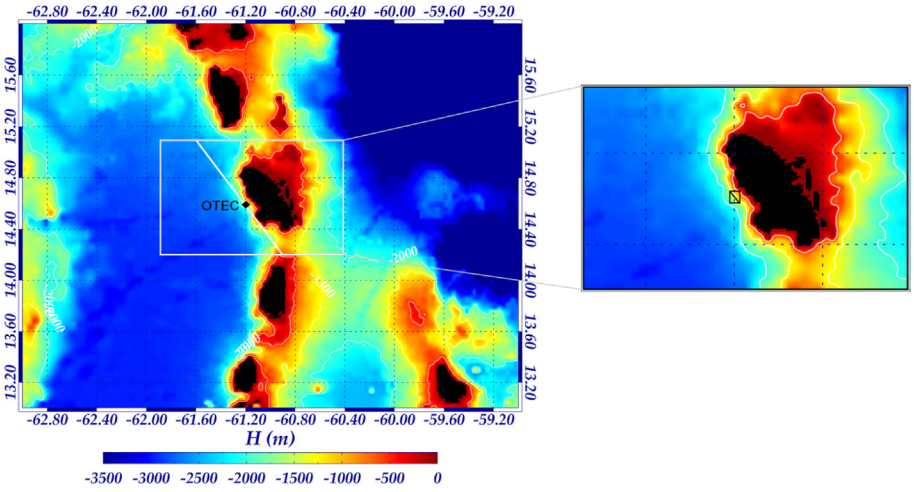

Fig. 1. Bathymetry of the parent and child (grey rectangle) domains interpolated from the GINA data base with a zoom on the near domain (black rectangle); the oblique white and black lines represent the large and small sections, respectively, used for numerical simulations.

Table 1
Comparison of analyses of SAFe (Sampling and Analysis of iron) S and D2 reference samples (http://www.geotraces.org/science/intercalibration) between ID-ICPMS values (this study) and the consensus values. Our mean reagent blanks (based on all blank determinations) for dissolved Cd, Pb, Fe, Ni, Cu, Zn, Mn and Co, and detection limits of ID-ICPMS estimated as three times the standard deviation of the mean reagent blanks are also shown.

	Cd (pM)	Pb (pM)	Fe (nM)	Ni (nM)	Cu (nM)	Zn (nM)	Mn (nM)	Co (pM)
SAFe D2								
This study	948.83 ± 65.95	28.86 ± 4.44	0.898 ± 0.098	8.60 ± 0.36	2.15 ± 0.16	7.29 ± 0.27	0.40 ± 0.05	40.12 ± 3.88
Consensus values	986.00 ± 23.00	27.70 ± 1.50	0.933 ± 0.023	8.63 ± 0.25	2.28 ± 0.15	7.43 ± 0.25	0.35 ± 0.05	45.70 ± 2.90
n=	20	20	18	19	22	13	23	23
SAFe S								
This study	7.24 ± 1.57	48.42 ± 6.08	0.087 ± 0.025	2.56 ± 0.55	0.55 ± 0.06	0.07 ± 0.06	0.75 ± 0.05	2.85 ± 0.81
Consensus values	1.10 ± 0.30	48.00 ± 2.20	0.093 ± 0.008	2.28 ± 0.09	0.52 ± 0.05	0.07 ± 0.01	0.79 ± 0.06	4.80 ± 1.20
n=	25	27	15	25	30	10	27	28
Detection limit	0.996	0.613	0.032	0.096	0.011	0.129	0.001	0.07
Blanks	0.716	1.809	0.061	0.040	0.019	0.129	0.003	0.32

Biovolume of each species was also estimated from these microscope analyses (Hillebrand et al., 1999).

2.2.2. In situ microcosm experiments

The potential impact of deep seawater discharge on the phytoplankton community was simulated by *in situ* microcosm incubations of various deep and surface seawater mixing (Giraud et al., 2016). The experiments were conducted from 12th (D0) to 19th (D7) of June 2014. The deep and surface seawaters were collected at the site of the future OTEC pilot plant (61°11′52″ W-14°37′57″ N; Fig. 1). Microcosms bottles were incubated on two stainless steel structures set at the depths of deep chlorophyll-*a* maximum (DCM) and at the bottom of the euphotic layer (BEL) on a mooring chain located, for practical reasons, closer to the coast (61°10′9″ W-14°39′8″ N, seafloor at 220 m depth) during 6 days (Giraud et al., 2016). This incubation time was chosen to represent the short-term phytoplankton response time to a mixing of deep water with surface waters. This duration is shorter or equal than the residence time of the enriched water mass, which is less than one month.

Seawater was collected at D0 at the depths of DCM (45 m depth) and BEL (80 m depth) identified on the future OTEC site from the fluorescence profile, and close to the bottom (1100 m depth corresponding to the pumping depth of the future OTEC plant) in ultra-clean conditions. Deep seawater was mixed in three proportions (0% as a control hereafter referred to as "Control", 2% as a low input called "2 % of deep seawater", and 10% as a large input called "10 % of deep seawater") with DCM and BEL waters. Each resulting mixture was distributed in 2.3 L polycarbonate bottles filled up to overflow level, of which four replicates per mixing condition per depth were immersed at their respective sampling-depth for 6 days; duplicates per mixing condition per depth were kept in dark at 25 °C for a few hours until sampling for later characterization of phytoplankton assemblage and biogeochemical properties at D0 (called "Surrounding waters D0"); and duplicates per mixing condition per depth were used to estimate carbon and NO_3^- uptakes at D0 (called "Surrounding waters D0") as described below.

Same sampling and mixtures were realized at day 6 (D6, June 18th) just to evaluate the temporal evolution in the natural environment, resting on duplicate bottles per mixing condition per depth for phytoplankton and biogeochemical characterizations at D6 (called "Surrounding waters D6") and using other duplicates to estimate carbon and NO_3^- uptakes at D6 (called "Surrounding waters D6").

After the 6 days incubation, all the incubated microcosm bottles on the mooring (called "Microcosm D6") were brought on board. A quarter of each four replicates per condition was put in a new 2.3 L clean bottle and used to estimate carbon and NO_3^- uptakes after 6 days of incubation (called "Microcosm D6"). The remaining microcosm contents were kept for sampling and analysis.

2.2.3. Carbon and nitrate uptakes

Carbon (primary production) and NO_3^- uptake rates were estimated in the same sample using the dual $^{13}C/^{15}N$ isotopic label technique (Slawyk et al., 1977). Immediately after sampling, ^{13}C tracer ($NaH^{13}CO_3$, 99 atom%, Eurisotop, 0.25 $mmol^{13}C.mL^{-1}$) and ^{15}N tracer ($Na^{15}NO_3$, 99 atom%, Eurisotop, 1 $\mu mol^{15}N.mL^{-1}$) were added to seawater mixtures at 10^{-3}:1 *v*/v ratio. The initial enrichment was 10 atom% excess of ^{13}C for the bicarbonate pool and 16–95 atom% excess of ^{15}N for the NO_3^- pool depending on the ambient NO_3^- concentration. The $^{13}C/^{15}N$ amended bottles were incubated for 24 h on the mooring line at the DCM and BEL depths, after which 1 L samples were filtered onto pre-combusted (450 °C, 4 h) glass fiber filters (Whatman). Filters were stored at −20 °C and oven dried (60 °C, 24 h) prior to analysis. Concentrations of carbon (POC), nitrogen (PON) as well as ^{13}C and ^{15}N enrichments in particulate matter were measured with a mass spectrometer (Delta plus, ThermoFisher Scientific) coupled to a C/N analyzer (Flash EA, ThermoFisher Scientific). Standard deviations were 0.009 μM and 0.004 μM for POC and PON, and 0.0002 atom% and 0.0001 atom% for ^{13}C- and ^{15}N-enrichments, respectively.

The absolute uptake rates (ρ, in $\mu mol.L^{-1}.h^{-1}$) were calculated for nitrogen (Dugdale and Wilkerson, 1986) and carbon (Fernández et al., 2005) using the particulate organic concentrations measured after 24 h of incubation. These rates were converted into biomass specific uptake rates (V_C or V_{NO3^-}, in $\mu mol.(\mu g\ Chl\ a)^{-1}.h^{-1}$) by dividing ρ by the total chlorophyll *a* concentration (TChl *a* defined as the sum of chlorophyll *a* and divinyl chlorophyll *a*) measured at the end of the incubations. The addition of ^{15}N tracer would cause a substantial increase in dissolved inorganic nitrogen concentrations especially in the surface waters and, in turn, an overestimation of uptake rates (Dugdale and Wilkerson, 1986; Harrison et al., 1996). The NO_3^- uptake rates were corrected for this perturbation (Dugdale and Wilkerson, 1986) using a half-saturation constant of 0.05 $\mu mol.L^{-1}$ characteristic for nitrogen-poor oceanic waters (Harrison et al., 1996) and the measured NO_3^- concentration. Overestimation was low (<5%) in samples with an addition of deep seawater but it was of about 50% in samples without deep seawater addition. The uptake rates measured in these samples represented therefore estimations rather than actual values.

2.2.4. Statistical analyses

Kruskal-Wallis test was applied on the set of pigments concentrations, pico-phytoplankton abundances and macronutrients concentrations. If significant differences ($p < 0.05$) were found, Mann-Whitney test was run to identify the samples significantly different. Statistical analyses were performed using Statgraphics Centurion XVI software.

3. Results

3.1. Impact of the deep seawater discharge on the thermal and density structure in surface

The representation of the thermocline and halocline depths, key proxies for oceanic mixing and for estimating the thermal impact of the OTEC discharge, is well mimicked over the 2 months (June and November) of the mesoscosm experiments (Giraud, 2016). In order to

assess the deep seawater discharge impact on the thermal structure of the upper 150 m of the water column, the dispersion of temperature differences (ΔT in °C) obtained without and with the deep seawater discharge in the model outputs was examined on two vertical sections. A section of 124 km for the large domain (corresponding to the child domain) and another section of 10 km for the near-OTEC domain (defined from 61.24° W to 61.17° W and 14.60° N to 14.67° N) were defined, both centered on the OTEC site and parallel to the coast (Fig. 1).

Presently, there are no environmental standards defining threshold levels for temperature difference that will be induced by an OTEC deep seawater discharge. So, the study relied on the World Bank Group prescriptions for liquefied natural gas facilities which set at 3 °C the temperature difference limit at the edges of the zone where initial mixing and dilution take place (IFC, 2007). We thus considered for each discharge depth the cooling and warming outputs from the model, which exhibit a $|\Delta T| \geq 3$ °C. Areas (in % of the considered domain) impacted by these cooling and warming effects were added (absolute values) in order to compare the potential impact of each discharge depth configuration. None of the discharge depth configurations could produce a modification of the thermal structure of the top 150 m of the water column, higher than or equal to the considered temperature threshold ($|\Delta T| \geq 3$ °C), for both domain sections.

Then, a lower temperature difference of 0.3 °C (absolute value) was considered. This temperature difference represented a low threshold as compared to the World Bank Group prescriptions (IFC, 2007) that instead represent a high threshold. The areas exhibiting a $|\Delta T| \geq 0.3$ °C in the top 150 m (Table 2) were extremely small (<1 km^2) and were not significantly different in both sections and at the different discharge depths, on an annual average and in June (our experimental period).

We also investigated the OTEC impact on density. The density of water being discharged at 45 m, depth of the deep chlorophyll maximum (DCM), is 27.48 (8 °C and salinity of 35). The density of water at 45 m is around 23.72 (temperature of 28 °C and salinity of 36.5) so the nominal density gradient is of 3.76. If one considers a modification of the density structure of the top 150 m of the water column of $|\Delta\rho| \geq 0.1$, there is no impact when the discharge occurs at the depth of the DCM. If one considers a lower density difference of 0.05 (absolute value), the area exhibiting a $|\Delta\rho| \geq 0.05$ in the top 150 m is extremely small (<1.5 km^2) in both sections at the depth of the chlorophyll maximum. As far as we know, there are no environmental standards defining threshold levels for density difference that will be induced by an OTEC deep seawater discharge. This represents <1.5% of the nominal density gradient so as for the thermal impact, the impact is estimated to be minor.

Table 2
Area (km^2) (average and root mean square) impacted in the top-150 m by a temperature difference $|\Delta T| \geq 0.3$ °C on two vertical sections centered on the OTEC, considering eight depths of deep seawater discharge (45, 80, 110, 140, 170, 250, 350, 500 m) (Giraud, 2016).

Depth of deep water discharge	Annual mean		June	
	Large domain	Near-OTEC domain	Large domain	Near-OTEC domain
45 m	0.4 ± 0.4	0.0 ± 0.1	0.0	0.0
80 m	0.6 ± 0.7	0.1 ± 0.1	0.4	0.0
110 m	0.6 ± 0.5	0.0 ± 0.1	0.9	0.0
140 m	0.4 ± 0.5	0.1 ± 0.1	0.1	0.0
170 m	0.5 ± 0.8	0.0 ± 0.1	0.5	0.0
250 m	0.5 ± 0.7	0.1 ± 0.1	0.1	0.0
350 m	0.5 ± 0.5	0.1 ± 0.1	0.0	0.0
500 m	0.5 ± 0.5	0.1 ± 0.1	0.3	0.0

3.2. Biogeochemical properties and phytoplankton community

3.2.1. Expected biogeochemical properties of the resulting mixed waters

The pH was very similar at the DCM and BEL at the OTEC site on D6 (8.24 and 8.25, respectively), whereas deep seawater-pH showed lower value (7.81). The addition of 2% and 10% deep seawater to surface waters could thus induce a pH-decrease of respectively, 0.01 and 0.07 unit. Hence, the effect on pH could be rather limited compared to the 0.1 pH decrease (from 8.2 to 8.1) between the pre-industrial time and the 1990's (Orr et al., 2005).

NO_3^- and PO_4^{3-} concentrations (Table 3) were below the detection limit (<0.02 μM) at the DCM (55 m) and BEL (80 m) at the OTEC site on observational D4 (June 16th 2014), whereas $Si(OH)_4$ concentrations were above detection limit (>0.08 μM), particularly at the DCM (2.4 μM). NO_2^- concentrations showed the highest values at the BEL whereas they were negligible at the DCM (<0.02 μM). In deep seawater, as commonly observed, NO_3^-, PO_4^{3-} and $Si(OH)_4$ concentrations were largely higher compared to the surface (Table 3). The 2% and 10% deep water additions represented a large input for NO_3^- in surface waters (from <0.02 μM to 0.54 and 2.71 μM, respectively; Table 3). If the 10% ratio also induced a large input of PO_4^{3-} (from <0.02 to 0.19 μM), the input of 2% deep water was more limited (0.04 μM). The effect of 2% or 10% deep seawater addition was more limited for $Si(OH)_4$ relatively to NO_3^- and PO_4^{3-} input, yet it accounted for 50–63% increase for 10% deep seawater addition (Table 3). Finally, because deep and DCM waters were NO_2^- depleted, the deep seawater input did not modify the NO_2^- concentration at the DCM. At the BEL, NO_2^- concentration was higher and the 10% addition slightly diluted NO_2^- at this depth.

Mn showed maximum concentrations in the surface layer on D4 at the OTEC site (Table 4) decreasing with depth as observed close to the Lesser Antilles in the Atlantic Ocean (Mawji et al., 2015), but the measured surface concentrations were particularly high, especially at the DCM. Fe that commonly dispatches hybrid distribution combining a nutrient-type profile in surface waters and a scavenged-type distribution in deep waters (Bruland, 2003) also exhibited high surface values, particularly at the DCM (Table 4). Cd, Zn, Co, Ni, and Cu dispatched nutrient-type profiles, whereas Pb exhibited scavenged-type profile (Nozaki, 1997; Gruber, 2008), but like for dissolved Fe and Mn, their concentrations in the upper waters were particularly high (Table 4). For all trace metals at both depths, the 2% deep seawater addition will not induce significant changes in their surface concentrations (Table 4). The 10% deep seawater addition could increase Cd, Ni and Zn concentrations in surface waters (Table 4), whereas it would not constitute an input of Pb, Cu, Co, and Fe, and it can even dilute Mn (Table 4).

The surface waters can thus be enriched in macronutrients (NO_3^-, PO_4^{3-}) when submitted to a deep seawater discharge (particularly with 10% deep seawater addition) in proportion depending on the

Table 3
Nitrate, silicate, phosphate and nitrite concentrations on June 16th 2014 (D4) at the deep chlorophyll maximum (DCM), at the bottom of the euphotic layer (BEL), and at the deep seawater pumping depth. Concentrations were measured at the OTEC site (0% addition of deep waters) and calculated for 2% and 10% deep seawater additions.

Depth (m)	Deep seawater ratio	[NO_3^-] (μM)	[$Si(OH)_4$] (μM)	[PO_4^{3-}] (μM)	[NO_2^-] (μM)
DCM	0%	<0.02	2.39	<0.02	0.02
	2%	0.54	2.88	0.04	0.02
	10%	2.71	4.82	0.19	0.02
BEL	0%	<0.02	1.46	<0.02	0.32
	2%	0.54	1.96	0.04	0.32
	10%	2.71	3.98	0.19	0.29
1100	100%	27.11	26.69	1.87	<0.02

Table 4
Concentrations of dissolved trace metals (in nM): Mn, Fe, Cd, Zn, Co, Ni, Cu, Pb measured on June 16th 2014 (D4) at the OTEC site at the DCM, BEL and 1100 m (0% addition of deep waters), and their calculated concentrations in the mixtures with 2% and 10% addition of deep water.

Depth (m)	Deep seawater ratio	Mn (nM)	Fe (nM)	Cd (nM)	Zn (nM)	Co (nM)	Ni (nM)	Cu (nM)	Pb (nM)
DCM	0%	2.97 ± 0.17	1.08 ± 0.03	0.03 ± 0.01	1.54 ± 0.04	0.05 ± 0.00	2.22 ± 0.10	1.70 ± 0.18	0.03 ± 0.00
	2%	2.92	1.08	0.04	1.56	0.05	2.29	1.70	0.03
	10%	2.71	1.09	0.07	1.63	0.05	2.60	1.71	0.03
BEL	0%	1.65 ± 0.04	0.68 ± 0.03	0.03 ± 0.00	0.65 ± 0.03	0.03 ± 0.00	2.26 ± 0.17	1.14 ± 0.10	0.03 ± 0.00
	2%	1.63	0.69	0.04	0.68	0.03	2.34	1.15	0.03
	10%	1.52	0.73	0.08	0.82	0.03	2.64	1.21	0.03
1100	100%	0.34 ± 0.02	1.22 ± 0.05	0.45 ± 0.01	2.39 ± 0.07	0.06 ± 0.00	6.00 ± 0.13	1.80 ± 0.08	0.02 ± 0.00

depth. The same scheme can be applied in some of the dissolved trace metals (Cd, Ni, Zn) when a large ratio of deep seawater (10%) is discharged.

3.2.2. Phytoplankton community in the natural environment

A set of seven accessory pigments identified as biomarkers of specific taxa (Uitz et al., 2010; Table 5) were analyzed at OTEC station at D0, D4 and D6 in surrounding surface waters (Fig. 2), as well as population abundance and their biovolume using light microscopy (Fig. 3).

TChl *a*, a proxy of the phytoplankton biomass, was higher at DCM than at BEL, as usually observed, by about two-folds. The fucoxanthin (biomarker of diatoms) concentrations were similar at the DCM and BEL on D0 (Fig. 2), like the total abundance of diatoms (Fig. 3). Fucoxanthin concentration increased by D4 and then by D6 at the DCM, corresponding to increases of cumulated diatoms biovolume on D4 (Fig. 3) and of diatoms abundance on D6 (Fig. 3). Peridinin, a biomarker of dinoflagellates, was detected at the DCM unlike at the BEL, with relatively high abundance and biovolume of dinoflagellates (Fig. 3). The 19′-hexanoyloxyfucoxanthin (biomarker of haptophytes) concentration (Fig. 2) and the prymmnesiophytes (haptophyte) abundance and biovolume (Fig. 3) showed higher values at the DCM than at the BEL only at D4.

At the DCM, dinoflagellates largely dominated the nano- and microphytoplankton assemblage with the largest abundance and biovolume. Whereas prymnesiophytes showed the second highest abundance, its biovolume was very low, on the contrary to diatoms that dispatched lower abundance but higher biovolume (Fig. 3). At the BEL, dinoflagellates, prymnesiophytes and diatoms showed similar abundance, dinoflagellates and the diatoms occupied the major part of the total biovolume. Three groups of dinoflagellates were observed by light microscopy but they could not be identified at species level. However, their small size and the lack of colored starch (using lugol) in the cytoplasm suggested they were mixotrophic or heterotrophic population. Furthermore, the low concentrations of peridinin in samples supported this assumption.

At both depths, light microscopy analyses suggested that the large cyanobacteria, mainly *Trichodesmium sp*., were low in abundance and biovolume. Flow cytometry identification and count indicated that the small cyanobacteria *Prochlorococcus* dominated the pico-phytoplankton assemblage, but they showed a significant decrease from D0 to D6 (Fig. 4). A significant portion of *Synechococcus* was also observed while picoeukaryotes were poorly represented. Both *Prochlorococcus* and *Synechococcus* showed higher abundance at the DCM than at the BEL (by 65% and 86%, respectively), in line with the pigment analyses of zeaxanthin (biomarker of cyanobacteria) and total chlorophyll *b* concentrations (prochlorophytes).

Table 5
Definition of the diagnostic pigments used as phytoplankton biomarkers (taxonomic significance) and associated phytoplankton size class (Uitz et al., 2010).

Diagnostic pigments	Abbreviations	Taxonomic significance	Phytoplankton size class
Fucoxanthin	Fuco	Diatoms	Microplankton
Peridinin	Perid	Dinoflagellates	Microplankton
19′-hexanoyloxyfucoxanthin	Hex-fuco	Haptophytes	Nanoplankton
19′-butanoyloxyfucoxanthin	But-fuco	Pelagophytes and Haptophytes	Nanoplankton
Alloxanthin	Allo	Cryptophytes	Nanoplankton
chlorophyll *b* + divinyl chlorophyll *b*	TChlb	Cyanobacteria, Prochlorophytes	Picoplankton
Zeaxanthin	Zea	Chlorophytes, Prochlorophytes	Picoplankton

3.2.3. Primary production and nitrate uptake in the natural environment

The phytoplankton distribution and assemblage can partly drive the intensity of primary production, so the specific uptake rate of carbon (V_C; Fig. 5) and NO_3^- (V_{NO3-}) were estimated at D0 and D6.

V_C in surrounding surface waters was relatively low at D0 (Fig. 5) indicating low primary production in these poor-nutrients waters. Yet, V_C was approximately three-times higher at the DCM (0.058 μmol C.(μg Chl *a*)$^{-1}$.h^{-1}) than at the BEL (0.017 μmol C.(μg Chl *a*)$^{-1}$.h^{-1}) at D0, but drastically decreasing on D6 at the DCM (to ~0.014 μmol C.(μg Chl *a*)$^{-1}$.h^{-1}). V_{NO3-} were also very low at D0 (0.014 μmol N.(μg Chl *a*)$^{-1}$.h^{-1} at DCM, 0.017 μmol N.(μg Chl *a*)$^{-1}$.h^{-1} at BEL) and drastically decreased at D6, below the detection limit (data not shown).

3.3. Impacts on the phytoplankton community of the deep seawater discharge

3.3.1. Changes in the phytoplankton assemblage

At the DCM, TChl *a* was similar in all treatments ($p < 0.05$) after 6 days of incubation in microcosms (Fig. 6). Only fucoxanthin and 19′-butanoyloxyfucoxanthin showed significant ($p < 0.05$) higher concentrations in 10% enrichments as compared to controls, indicating higher abundance and/or biovolume of diatoms and haptophytes. The other diagnostic pigments did not show any significant difference between enriched microcosms and controls. Picoeukaryotes and *Synechococcus* abundances did not show significant variations between the treatments (Fig. 7a). Reversely, *Prochlorococcus* population showed higher ($p < 0.05$) abundance both in 2% and 10% enriched microcosms as compared to controls (Fig. 7a).

At the BEL, after the 6 days incubation period, pigments concentrations were below the detection limit indicating very low abundance of phytoplankton. Pico-phytoplankton did not show significant variations between the treatments and the controls (Fig. 7b). Pico-phytoplankton were clearly much less abundant at the BEL (<1000 cells.mL^{-1}) than at DCM (Fig. 7b), 20-times even lower than that observed in surrounding waters at this depth on D6. For comparison, total abundance at the DCM was ~5-times lower in incubated microcosms on D6 compared to surrounding surface waters.

3.3.2. Changes in the primary production and nitrate uptake

Deep water inputs (2% and 10%) to surrounding waters collected at the DCM on D0 led to an increase of V_C within 24 h compared to the controls (by 42% and 49%, respectively; Fig. 5); but they had no effect on D6 despite very low value in natural waters at this depth (0.014 μmol N.(μg Chl *a*)$^{-1}$.h^{-1}). The 6 days incubated microcosms showed very low V_C in all treatments (Fig. 5). At the BEL, V_C were quite similar on D0 and D6 and after 6 days of incubation. Vc increased by 57% with 10% addition

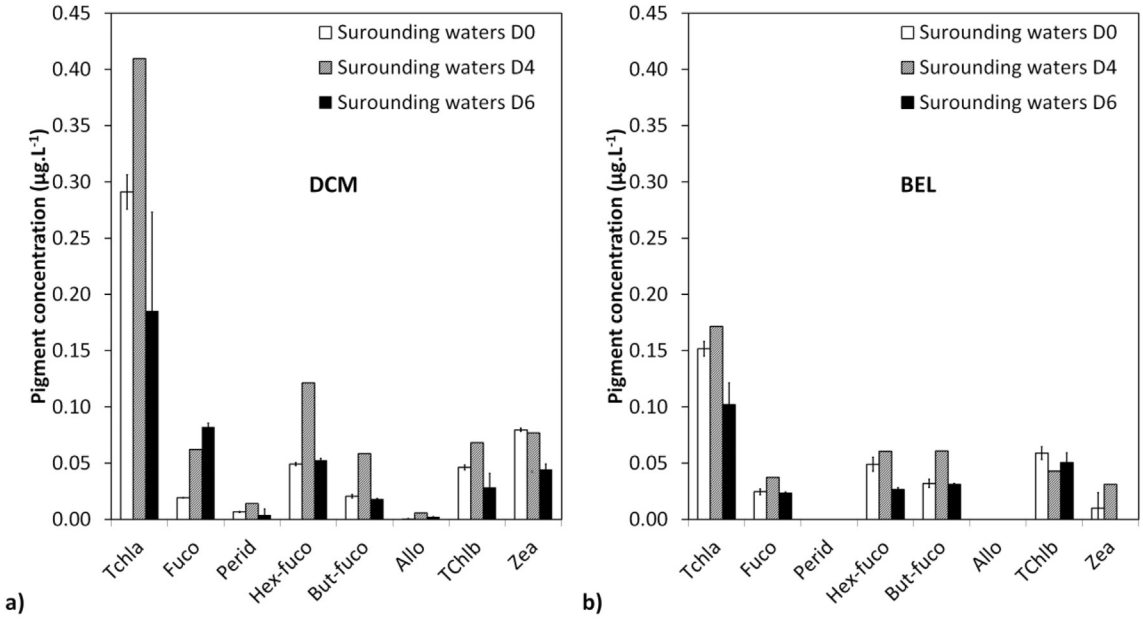

Fig. 2. Pigment concentrations (from HPLC analysis) at the OTEC site at the DCM (a) and at the BEL (b), on June 12th (D0), 16th (D4), 18th (D6) 2014 (bars represent the standard deviation).

of deep water on Do and was approximately two times higher than the control with the two enrichments on D6 (Fig. 5). V_{NO3^-} measured in microcosms after a 6-days *in situ* incubation were below the detection limit (data not shown).

4. Discussion

4.1. Natural variabilities in the oligotrophic area

4.1.1. Biogeochemistry and phytoplankton community structure

The very low PO_4^{3-} and NO_3^- concentrations recorded in the oligotrophic surrounding surface waters were likely favorable to the development of small phytoplankton, especially to the cyanobacteria as shown with the significant occurrence of *Prochlorococcus* in these waters, which are typical of poor nutrient waters (Partensky et al., 1999). In line with the very low V_{NO3^-} measured here, it has been shown that V_{NO3^-} by *Prochlorococcus* represents indeed only 5–10% of its nitrogen uptake whereas reduced nitrogen substrates (NO_2^-, ammonium, and urea) uptake accounts for >90–95% (Casey et al., 2007). By contrast, the development of larger phytoplankton taxa (particularly diatoms), which have higher NO_3^- and PO_4^{3-}requirements for their growth, were probably limited by these elements. Actually, NO_3^- and PO_4^{3-} concentrations in surrounding waters at the DCM were both lower than the detection limit (<0.02 μM at D4) which is much lower than the average values of half-saturation constants for diatoms (1.6 ± 1.9 μM for NO_3^- and 0.24 ± 0.29 μM for PO_4^{3-}; Sarthou et al., 2005). For $Si(OH)_4$, surrounding surface concentrations at DCM (2.39 μM) were in the range of diatoms half-saturation constants (3.9 ± 5.0 μM; Sarthou et al., 2005), hence the diatoms development was probably not limited by $Si(OH)_4$. Furthermore, diatoms showed low abundance in spite of relatively high $Si(OH)_4$ and dissolved trace metals (in particular Fe) concentrations in surface waters. The potential of Fe limitation on phytoplankton community has been reported previously in upwelling systems, with an apparent half-saturation constant for diatoms growth of 0.26 nM Fe in the Peru Upwelling system (Hutchins et al., 2002). This constant is far lower than the concentration of Fe measured in surrounding waters at DCM (1.08 ± 0.03 μM at D4), suggesting that diatoms were probably not limited by Fe. This further supports growth limitation of diatoms by NO_3^- and/or PO_4^{3-}.

Advection of waters from Amazon and Orinoco rivers can explain the relatively high $Si(OH)_4$ observed in the Caribbean Sea. However, little information is available on the input of trace metals by these waters into the Caribbean Sea. Amazon river can be a source of dissolved Fe, Cu, Ni, Pb and Co for the western-subtropical North Atlantic (Tovar-Sanchez and Sañudo-Wilhelmy, 2011), but this input can decrease rapidly away from its source like it has been shown for Co in the Western Atlantic (Dulaquais et al., 2014). Those inputs into the Caribbean Sea will have to be further examined, especially for Fe, Cd, Ni, Zn, Mn whose relatively high concentrations were detected in the Si $(OH)_4$-enriched surface waters of this study. Additionally, other inputs of trace metals such as atmospheric deposition can also increase surface concentrations, and those inputs can be substantial (Shelley et al., 2012).

4.1.2. Primary production

Primary production rates measured in the oligotrophic surrounding waters were in the lower range of values reported for oligotrophic waters (Laws et al., 2016; Teira et al., 2005). Despite low V_C on D0 and D6 at the DCM, primary production still indicated much higher value on D0 compared to D6 that was associated with higher TChl *a* (Fig. 2a). The decrease of divinyl-chlorophyll *a* concentration, a biomarker of *Prochlorococcus* (Goericke and Repeta, 1992), over the 6 days of observation can account for the decrease of TChl *a*, whereas chlorophyll *a* concentrations did not vary significantly during this period. The *Prochlorococcus* abundance was also lower by two-times on D6 compared to D0 (Fig. 4a). On the contrary, fucoxanthin (diatoms) increased by four-times over the 6 days (Fig. 2a), as well as the diatoms abundance (by three-times; Fig. 3a). In turn, the increase in diatoms abundance was not associated with an increase in primary production. Instead, the observed decrease in primary production can be due to the decrease in *Prochlorococcus* abundance. In tropical and subtropical waters, pico-phytoplankton can indeed contribute to >80% of the primary production (Platt et al., 1983; Goericke and Welschmeyer, 1993). The development of diatoms population likely did not compensate the large decrease in *Prochlorococcus* abundance (from 141,000 to 63,000 cells.mL^{-1}).

4.2. Impact of deep seawater discharge

4.2.1. Temperature effects

The numerical simulation showed that the area impacted in the top-150 m by a temperature difference larger than or equal to 0.3 °C

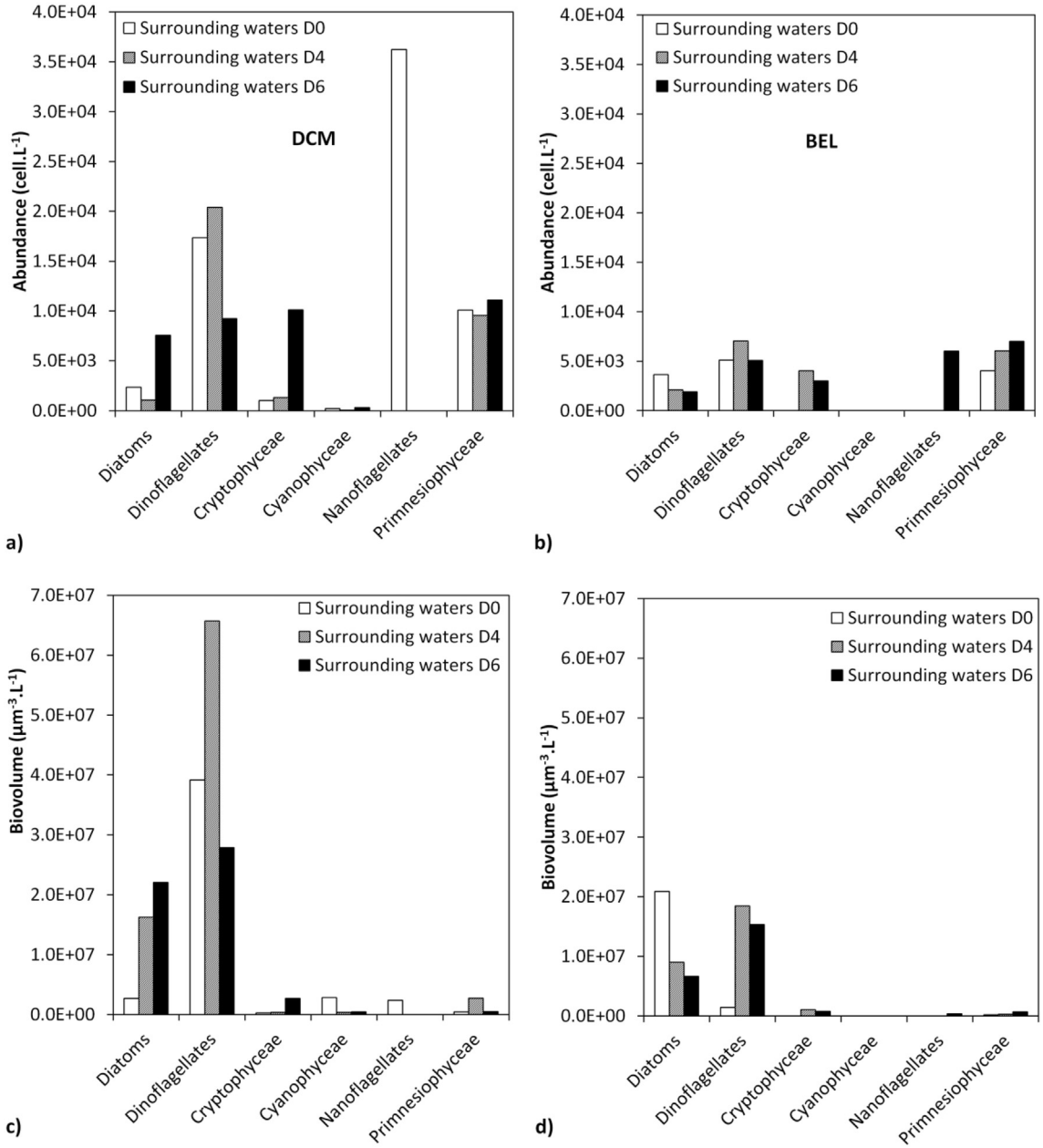

Fig. 3. Abundance and biovolume of micro- and part of nano-phytoplankton at the OTEC site on June 12th (D0), 16th (D4), 18th (D6) 2014, at the DCM (a and c, respectively) and at the BEL (b and d, respectively) (bars represent the standard deviation).

(absolute value) was lower than 1 km^2 (~2–3% of the considered domain) and was insensitive to the injection depth or to the size of the tested domain (Table 2). The impact of a 0.3 °C temperature variation on the growth of diatoms, notably on *Pseudonitzschia pseudodelicatissima* species that were observed in our study area, is limited to a change in the growth rate of 0.03 d^{-1} (Lundholm et al., 1997). For *Synechococcus*, a 0.3 °C variation of the temperature would also have a limited impact on the growth, with a variation of only 0.02 d^{-1} (Boyd et al., 2013), like for *Emiliania huxleyi* (coccolithophyceae) for which the induced variation of maximum growth rate will be lower than 0.01 d^{-1} (Fielding, 2013). The thermal effect on the phytoplankton assemblage could thus be considered negligible.

4.2.2. Impact on the phytoplankton community

Microcosms enrichment of DCM waters with 10% of deep seawater led after 6 days to a significant increase ($p < 0.05$) of fucoxanthin (diatoms) and 19′-butanoyloxyfucoxanthin (haptophytes) by 71% and 77%, respectively, as compared to the controls. If the 2% enrichment also showed similar trends, the differences of diagnostic pigments concentrations were not significant. NO_3^- and PO_4^{3-} concentrations induced by 10% deep-water input on D0 (2.57 ± 0.13 µM and 0.14 ± 0.2 µM, respectively; Giraud et al., 2016) were close to NO_3^- and PO_4^{3-} half-saturation constants of diatoms (1.6 ± 1.9 µM and 0.24 ± 0.29 µM, respectively; Sarthou et al., 2005). The 10% enrichment could thus support a development of diatoms. On the contrary, NO_3^- and PO_4^{3-} enrichments induced by 2% addition of deep-water were too low (0.57 ± 0.02 µM and 0.04 ± 0.00 µM, respectively; Giraud et al., 2016) compared to these half-saturation constants to support the diatoms development. Therefore, the diagnostic pigments suggested a significant response proportionally to the amount of added deep seawater.

Prochlorococcus were also more abundant ($p < 0.05$) in 2% and 10% treatments as compared to the controls. This lack of further *Prochlorococcus* population increase in 10% treatments could be

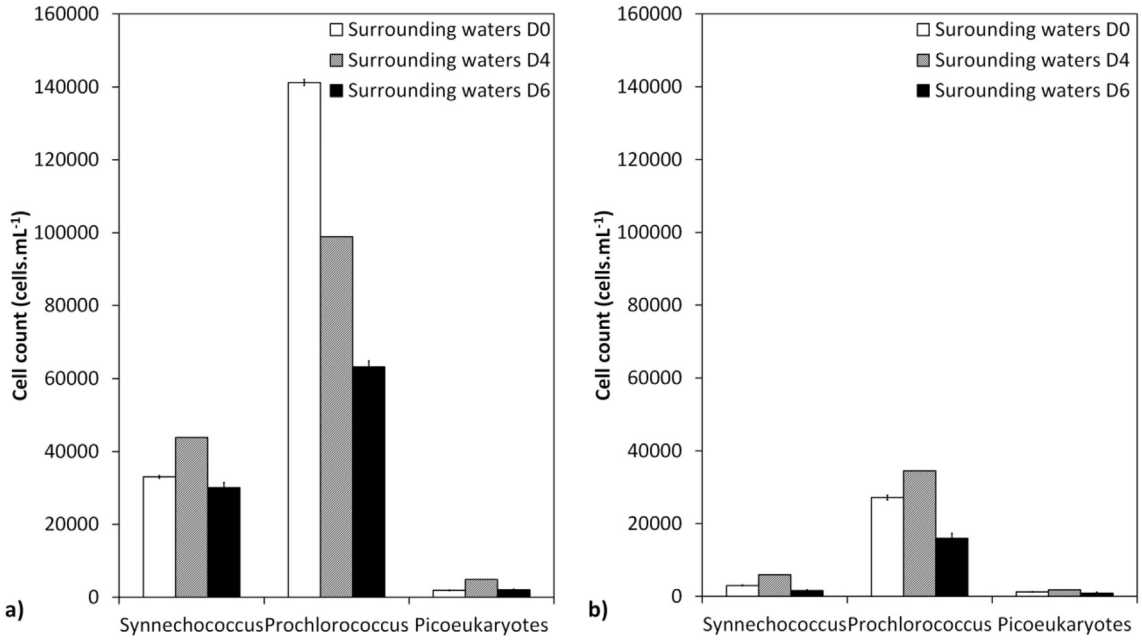

Fig. 4. Abundance of pico-phytoplankton at the DCM (a) and at the BEL (b), on June 12th (D0), 16th (D4), 18th (D6) 2014 (bars represent the standard deviation).

attributed to a higher grazing pressure by haptophytes and/or to NO_3^- and PO_4^{3-} too rich conditions (Giraud et al., 2016).

Phytoplankton assemblage widely evolved in surrounding waters, from a predominance of pico-phytoplankton (*Prochlorococcus*) on D0 toward a higher abundance of micro-phytoplankton (diatoms) on D6. In order to assess if the impact on the phytoplankton assemblage due to 10% deep seawater addition (with a shift toward the diatoms) was in the range of the natural variation observed in the surrounding surface waters, 10% deep seawater microcosms phytoplankton assemblage was compared to the natural phytoplankton assemblage.

Whereas microcosm controls showed a lower *Prochlorococcus* abundance (Fig. 7a) than surrounding surface waters on D6 ($p < 0.05$), the 10% microcosms additionally showed, higher fucoxanthin (diatoms) and 19′-butanoyloxyfucoxanthin (haptophytes) by about 142% and 317% (Fig. 6), respectively, as compared to natural waters at D6. Furthermore, 10% enrichments showed a fucoxanthin increase over the 6 days period by 3-times higher than in surrounding waters, whereas controls only showed an increase by 1.5-times higher than in surrounding waters. Therefore, it can be concluded that the 10% deep seawater enrichment induced higher variations of the phytoplankton assemblage than those observed from D0 to D6 in surrounding surface waters.

V_C were higher ($p < 0.05$) both in 2% and 10% enrichments on D0 as compared to controls, suggesting a positive response of phytoplankton to the deep seawater addition. Conversely, there was no carbon-uptake rate difference ($p < 0.05$) between controls and enriched waters (with 2% and 10% of deep seawater) at D6 with the 6 days incubated

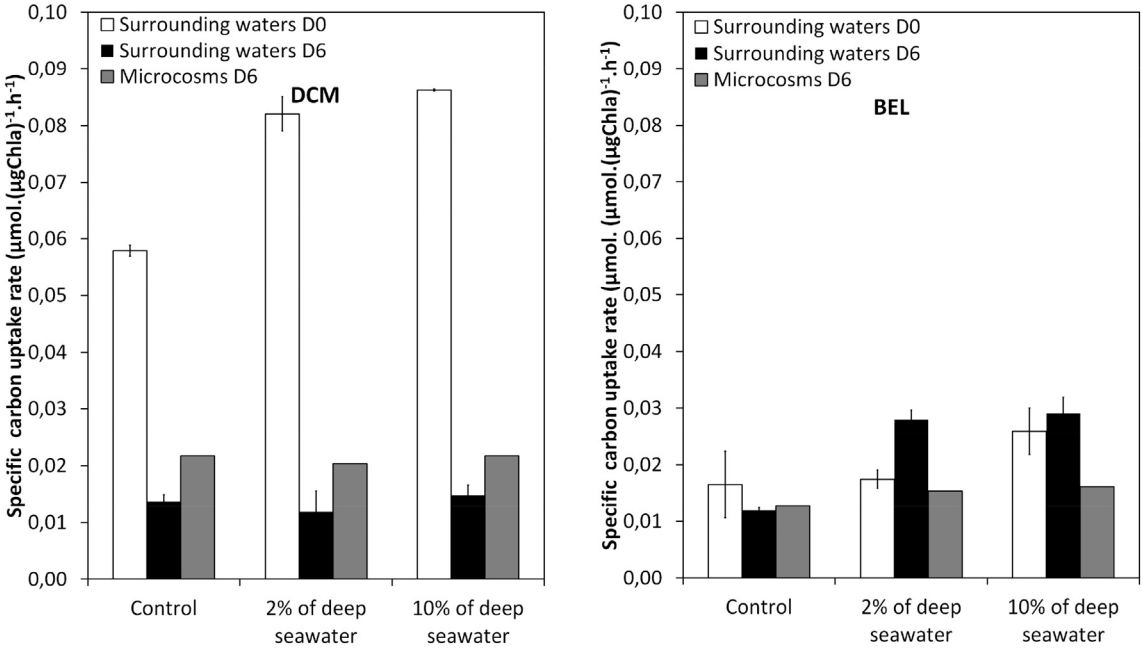

Fig. 5. Specific carbon uptake rate (µmol.(µg Chl *a*)$^{-1}$.h^{-1}) at the DCM (a) and BEL (b) depths, on June 12th (D0), and 18th (D6), and in 6 days incubated microcosms (D6), for the three mixing conditions (0%, 2% and 10% of deep seawater additions) (for surrounding waters bars represent the standard deviation for 2 replicates).

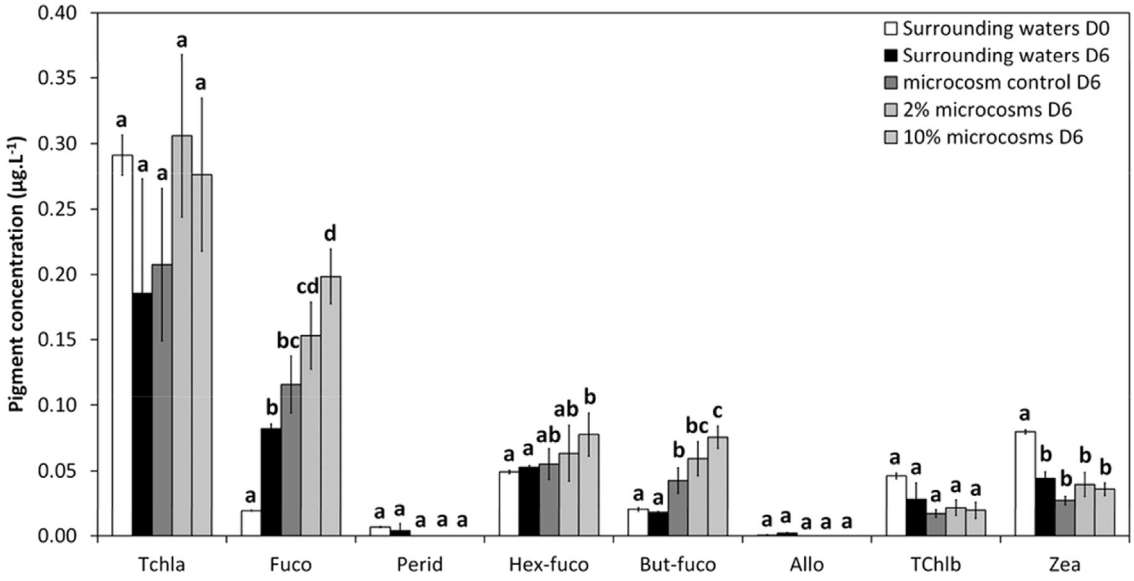

Fig. 6. Diagnostic pigment concentrations in surrounding surface waters on D0 and D6, and in controls and deep water-enriched (2% and 10%) microcosms after 6 days of incubation at the DCM (bars represent the standard deviation). Similar letters (a, b or c) attributed to 2 or more treatments indicate no significant differences ($p < 0.05$) between these treatments.

microcosms, suggesting that the observed community modifications did not change the primary production. Indeed, the phytoplankton community was quite similar in surrounding surface waters on D6 and in 6 days-incubated microcosm controls. Thus, only the initial phytoplankton assemblage and initial primary production in surrounding surface waters would influence the response of the phytoplankton community and its production.

At the BEL, after 6 days of incubation, deep seawater addition experiments clearly showed lower effects on the phytoplankton community than at the DCM. Indeed, whereas significant differences ($p < 0.05$) between 10% enrichments and controls were observed in diagnostic pigments concentrations at the DCM, pigments concentrations were too low at the BEL to be quantified. It can be suggested that the lower population and lower carbon uptake could be related to the lowest light availability.

Overall, the phytoplankton response was proportional to the amount of added deep seawater. If the phytoplankton assemblage significantly varied over time in the environment, the 10% deep seawater enrichment showed larger variations (for diatoms and haptophytes) than those observed in the natural environment. The DCM should be more impacted than the BEL by the deep seawater discharge even with a large deep seawater input. On the other hand, the impact on the primary production largely depended on the initial phytoplankton assemblage, which was quite variable over time. The modification of the phytoplankton community to a deep seawater input could also be depending on the initial phytoplankton community. For that, the microcosm experiments did not allow drawing a scenario over the long term of the potential modifications of the primary production and the phytoplankton community associated to the deep seawater discharge by an OTEC.

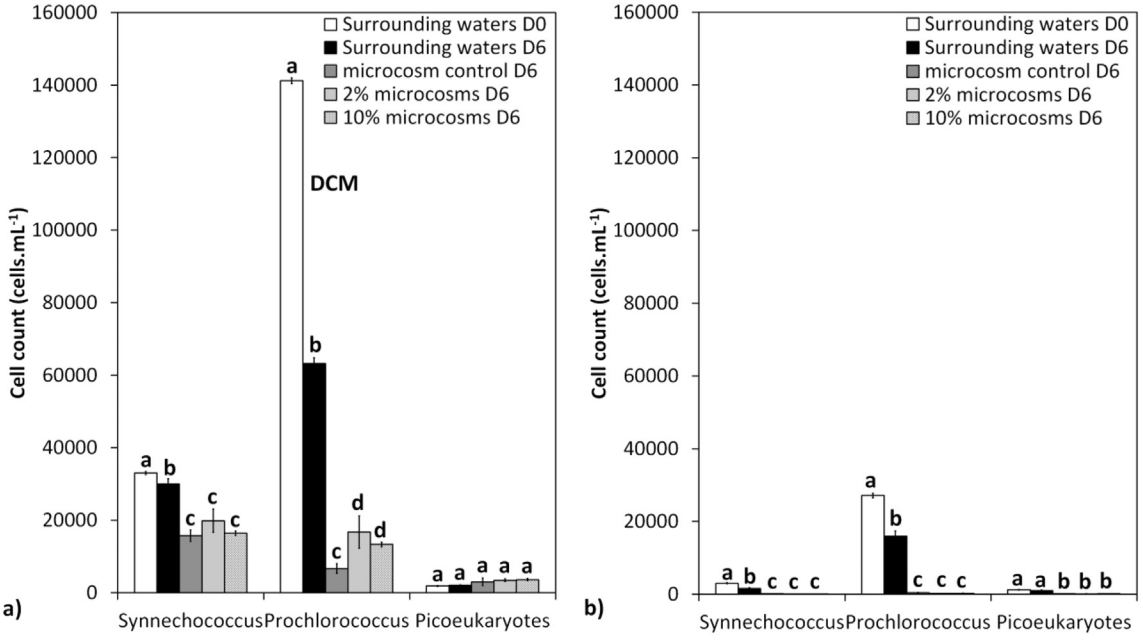

Fig. 7. Abundance of picophytoplankton in surrounding surface waters on days 0 and 6, and in controls and deep water-enriched (2% and 10%) microcosms after 6 days of incubation at 45 m depth (a) and 80 m depth (b) (bars represent the standard deviation). Similar letters (a, b or c) attributed to 2 or more treatments indicate no significant differences ($p < 0.05$) between these treatments.

Finally, light microscopy analyses showed a large abundance of dinoflagellates at the DCM (between 9240 and 20,400 cells.mL^{-1} on D6 and D4; Fig. 3a) which could be mixotrophic or heterotrophic and thus probably exert a grazing pressure on the phytoplankton, particularly on the pico-phytoplankton (Liu et al., 2002). However, in this study, the zooplankton larger than 200 μm and its potential control on the phytoplankton community were not considered and should be examined in future studies.

5. Conclusion

Two complementary approaches were applied to study the potential effects of the deep seawater discharge of the planned OTEC plant on the phytoplankton community in oligotrophic waters off Martinique.

Because the distribution and the development of phytoplankton are directly linked to the surface stratification, it is important to assess the thermal effect of deep seawater by an OTEC plant. Modelling of the deep seawater discharge showed that the thermal structure of the top 150 m of the water column on large and near-OTEC sections should be very slightly impacted for the lowest considered temperature differences $|\Delta T| \geq 0.3$ °C. If World Bank Group prescriptions of not exceeding a higher temperature difference of 3 °C are followed, the environmental perturbations potentially caused by the operation of the OTEC should be considered negligible. The area where the 150 m-depth waters are impacted by the lowest considered temperature differences $|\Delta T| \geq 0.3$ °C would not exceed 1 km^2 in a worst-case scenario.

The phytoplankton community and its production could be impacted by a large deep seawater input. Whereas pico-phytoplankton currently largely dominates the phytoplankton assemblage, a ratio of 10% of deep seawater in DCM waters could induce a shift toward the diatoms and micro-phytoplankton. The ratio of 2% of deep seawater in DCM waters only showed significant higher *Prochlorococcus* abundance than controls, but the assemblage and the primary production were not modified by this lower input. The stimulation of *Prochlorococcus* could be due to one or some of the following causes: NO_3^- and/or PO_4^{3-} supply, trace metal supply, lowered pH (higher availability of dissolved inorganic carbon). Since the lower impact on the phytoplankton assemblage was obtained at BEL, this depth can be recommended for the discharge the deep seawater to exploit the OTEC plant.

Although significant, these results would have to be extended to larger temporal scale, and the phytoplankton interactions with higher trophic levels (such as zooplankton) must be studied.

Because no environment standards on the deep seawater discharge effects are available yet, a rigorous monitoring of the phytoplankton community, biogeochemical parameters distribution and of the water column stratification must be established as soon as the OTEC is implemented and during its continuous functioning.

Acknowledgements

This work was supported by France Energies Marines as part of the IMPALA project. We would like to thank the Captains and crew members of the "Pointe d'Enfer", and the scientists in the laboratory at the University of the French West Indies and Guiana at Martinique; Dominique Marie (UPMC, Roscoff, France) and Christophe Lambert (LEMAR, France) for their help with the flow cytometry, and Anne Donval (LEMAR, France) for the pigment analyses.

References

Agawin, N.S.R., Duarte, C.M., Agustí, S., 2000. Nutrient and temperature control of the contribution of picoplankton to phytoplankton biomass and production. Limnol. Oceanogr. 45 (8), 1891.

Aminot, A., Kérouel, R., 2007. Dosage automatique des nutriments dans les eaux marines: méthodes en flux continu. In: Ifremer (Ed.), Méthodes D'analyse en Milieu Marin, Quae.

Aure, J., Strand, O., Erga, S.R., Strohmeier, T., 2007. Primary production enhancement by artificial upwelling in a western Norwegian fjord. Mar. Ecol. Prog. Ser. 52, 39–470.

Bakun, A., 1990. Global climate change and intensification of coastal ocean upwelling. Science 247 (4939), 198–201.

Boyd, P.W., Jickells, T., Law, C.S., Blain, S., Boyle, E.A., Buesseler, K.O., et al., 2007. Mesoscale iron enrichment experiments 1993–2005: synthesis and future directions. Science 315 (5812), 612–617.

Boyd, P.W., Rynearson, T.A., Armstrong, E.A., Fu, F., Hayashi, K., Hu, Z., et al., 2013. Marine phytoplankton temperature versus growth responses from polar to tropical waters–outcome of a scientific community-wide study. PLoS One 8 (5), e63091.

Bruland, K.W., 2003. Controls on trace metals in seawater. The Oceans and Marine Geochemistry, Treatise on Geochemistry. 6, pp. 23–47.

Bruland, K.W., Rue, E.L., Smith, G.J., 2001. Iron and macronutrients in California coastal upwelling regimes: implications for diatom blooms. Limnol. Oceanogr. 46, 1661–1674.

Brzezinski, M.A., 1985. The Si:C:N ratio of marine diatoms. Interspecific variability and the effect of environmental variables. J. Phycol. 21, 347–357.

Carr, M.E., Kearns, E.J., 2003. Production regimes in four Eastern Boundary Current systems. Deep-Sea Res. II Top. Stud. Oceanogr. 50 (22), 3199–3221.

Carton, J.A., Giese, B.S., 2008. A reanalysis of ocean climate using Simple Ocean Data Assimilation (SODA). Mon. Weather Rev. 136 (8), 2999–3017.

Casey, J.R., Lomas, M.W., Mandecki, J., Walker, D.E., 2007. Prochlorococcus contributes to new production in the Sargasso Sea deep chlorophyll maximum. Geophys. Res. Lett. 34 (10).

Chavez, F.P., Toggweiler, J.R., 1995. Physical estimates of global new production: the upwelling contribution. In: Summerhayes, C.P., Emeis, K.C., Angel, M.V., Smith, R.L., Zeitzschel, B. (Eds.), Upwelling in the Ocean: Modern Processes and Ancient Records. Wiley, pp. 313–320.

De Baar, H.J., Boyd, P.W., Coale, K.H., Landry, M.R., Tsuda, A., et al., 2005. Synthesis of iron fertilization experiments: from the Iron Age in the age of enlightenment. J. Geophys. Res. Oceans 110 (C9).

Duarte, C.M., Agusti, S., Agawin, N.S.R., 2000. Response of a Mediterranean phytoplankton community to increased nutrient inputs: a mesocosm experiment. Mar. Ecol. Prog. Ser. 195, 61–70.

Dugdale, R.C., Wilkerson, F.P., 1986. The use of ^{15}N to measure nitrogen uptake in eutrophic oceans; experimental considerations. Limnol. Oceanogr. 31 (4), 673–689.

Dulaquais, G., Boye, M., Rijkenberg, M.J.A., Carton, X.J., 2014. Physical and remineralization processes govern the cobalt distribution in the deep western Atlantic Ocean. Biogeosciences 11 (6), 1561–1580.

Dussart, B.M., 1966. Les différentes catégories de plancton. Hydrobiologia 26, 72–74.

Escaravage, V., Prins, T.C., Smaal, A.C., Peeters, J.C.H., 1996. The response of phytoplankton communities to phosphorus input reduction in mesocosm experiments. J. Exp. Mar. Biol. Ecol. 198, 55–79.

Fernández, I., Raimbault, P., Garcia, N., Rimmelin, P., Caniaux, G., 2005. An estimation of annual new production and carbon fluxes in the northeast Atlantic Ocean during 2001. J. Geophys. Res. Oceans 110 (C7) (1978–2012). C07S13.

Fielding, S.R., 2013. *Emiliania huxleyi* specific growth rate dependence on temperature. Limnol. Oceanogr. 58 (2), 663–666.

Giraud, M., 2016. Evaluation de L'impact Potentiel d'un Upwelling Artificiel lié au Fonctionnement D'une Centrale à Énergie Thermique des Mers sur le Phytoplancton. Doctorat de l'Université de Bretagne Occidentale, 150 p. .

Giraud, M., Boye, M., Garçon, V., Donval, A., De La Broise, D., 2016. Simulation of an artificial upwelling using immersed in situ phytoplankton microcosms. J. Exp. Mar. Biol. Ecol. 475, 80–88.

Goericke, R., Repeta, D.J., 1992. The pigments of *Prochlorococcus marinus*: the presence of divinyl chlorophyll a and b in a marine prochlorophyte. Limnol. Oceanogr. 37, 425–433.

Goericke, R., Welschmeyer, N.A., 1993. The marine prochlorophyte *Prochlorococcus* contributes significantly to phytoplankton biomass and primary production in the Sargasso Sea. Deep-Sea Res. I Oceanogr. Res. Pap. 40 (11), 2283–2294.

Gruber, N., 2008. The marine nitrogen cycle: overview and challenges. Nitrogen in the Marine Environment, pp. 1–50.

Handå, A., McClimans, T.A., Reitan, K.I., Knutsen, Ø., Tangen, K., Olsen, Y., 2014. Artificial upwelling to stimulate growth of non-toxic algae in a habitat for mussel farming. Aquac. Res. 45, 1798–1809.

Harrison, W.G., Harris, L.R., Irwin, B.D., 1996. The kinetics of nitrogen utilization in the oceanic mixed layer: nitrate and ammonium interactions at nanomolar concentrations. Limnol. Oceanogr. 41 (1), 16–32.

Hasle, G.R., 1988. The inverted microscope method. In: Sournia, A. (Ed.), Phytoplankton Manual. UNESCO, Paris.

Hillebrand, H., Durselen, C.D., Kirchttel, D., Pollingher, U., Zohary, T., 1999. Biovolume calculation for pelagic and benthic microalgae. J. Phycol. 35, 403–424.

Hooker, S.B., Clementson, L., Thomas, C.S., Schlüter, L., Allerup, M., Ras, J., Claustre, H., et al., 2012. NASA Tech. Memo. 2012–217503. NASA Goddard Space Flight Center, Greenbelt, Maryland.

Hutchins, D.A., Hare, C.E., Weaver, R.S., Zhang, Y., Firme, G.F., DiTullio, G.R., Alm, M.B., Riseman, S.F., Maucher, J.M., Geesey, M.E., Trick, C.G., Smith, G.J., Rue, E.L., Conn, J., Bruland, K.W., 2002. Phytoplankton iron limitation in the Humboldt current and Peru upwelling. Limnol. Oceanogr. 47, 997–1011.

International Finance Corporation (IFC), 2007. World Bank Group, Environmental, Health, and Safety Guidelines for Liquefied Natural Gas (LNG) Facilities.

Kagaya, S., Maeba, E., Inoue, Y., Kamichatani, W., et al., 2009. A solid phase extraction using a chelate resin immobilizing carboxymethylated pentaethylenehexamine for separation and preconcentration of trace elements in water samples. Talanta 79 (2), 146–152.

Kress, N., Thingstad, T.F., Pitta, P., Psarra, S., Tanaka, T., Zohary, T., Groom, S., Herut, B., Mantoura, R.F.C., Polychronaki, T., Rassoulzadegan, F., Spyres, G., 2005. Effect of P and N addition to oligotrophic Eastern Mediterranean waters influenced by near-

shore waters: a microcosm experiment. Deep-Sea Res. II Top. Stud. Oceanogr. 52, 3054–3073.
Laws, E.A., Bidigare, R.R., Karl, D.M., 2016. Enigmatic relationship between chlorophyll a concentrations and photosynthetic rates at station ALOHA. Heliyon 2, e00156.
Liu, H., Suzuki, K., Saino, T., 2002. Phytoplankton growth and microzooplankton grazing in the subarctic Pacific Ocean and the Bering Sea during summer 1999. Deep-Sea Res. I Oceanogr. Res. Pap. 49 (2), 363–375.
Lundholm, N., Skov, J., Pocklington, R., Moestrup, Ø., 1997. Studies on the marine planktonic diatom *Pseudo-nitzschia*. 2. Autecology of *P. pseudodelicatissima* based on isolates from Danish coastal waters. Phycologia 36 (5), 381–388.
Marie, D., Partensky, F., Vaulot, D., Brussaard, C., 1999. Enumeration of phytoplankton, bacteria, and viruses in marine samples. Curr. Protoc. Cytom. 1–11.
Mawji, E., Schlitzer, R., et al., 2015. The GEOTRACES intermediate data product 2014. Mar. Chem. 177 (1), 1–8. https://doi.org/10.1016/j.marchem.2015.04.005.
Milne, A., Landing, W., Bizimis, M., Morton, P., 2010. Determination of Mn, Fe, Co, Ni, Cu, Zn, Cd and Pb in seawater using high resolution magnetic sector inductively coupled mass spectrometry (HR-ICP-MS). Anal. Chim. Acta 665 (2), 200–207.
National Oceanic and Atmospheric Administration (NOAA), 1981. Ocean Thermal Energy Conversion Final Environmental Impact Statement. Office of Ocean Minerals and Energy, Charleston, SC.
National Oceanic and Atmospheric Administration (NOAA), 2010. Ocean Thermal Energy Conversion: Assessing Potential Physical, Chemical, and Biological Impacts and Risks. University of New Hampshire, Durham, NH.
Nozaki, Y., 1997. A fresh look at element distribution in the North Pacific Ocean. Eos Trans. AGU 78 (21), 221.
Orr, J.C., Fabry, V.J., Aumont, O., Bopp, L., Doney, S.C., Feely, R.A., Gnanadesikan, A., Gruber, N., Ishida, A., Joos, F., Key, R.M., Lindsay, K., Maier-Reimer, E., Matear, R., Monfray, P., Mouchet, A., Najjar, R.G., Plattner, G.K., Rodgers, K.B., Sabine, C.L., Sarmiento, J.L., Schlitzer, R., Slater, R.D., Totterdell, I.J., Weirig, M.F., Yamanaka, Y., Yool, A., 2005. Anthropogenic ocean acidification over the twenty-first century and its impact on calcifying organisms. Nature 437 (7059), 681–686.
Partensky, F., Hess, W.R., Vaulot, D., 1999. *Prochlorococcus*, a marine photosynthetic prokaryote of global significance. Microbiol. Mol. Biol. Rev. 63 (1), 106–127.
Pauly, D., Christensen, V., 1995. Primary production required to sustain global fisheries. Nature 374 (6519), 255–257.
Platt, T., Rao, D.S., Irwin, B., 1983. Photosynthesis of picoplankton in the oligotrophic ocean. Nature 301, 702–704.
Rocheleau, G., Hamrick, J., Church, M., 2012. Modeling the Physical and Biochemical Influence of Ocean Thermal Energy Conversion Plant Discharges Into Their Adjacent Waters, Final Technical Report. U.S. Department of Energy Award N° DE-EE0003638, Makai Ocean Engineering, Inc, Kailua, Hawaii.
Sarthou, G., Timmermans, K.R., Blain, S., Tréguer, P., 2005. Growth physiology and fate of diatoms in the ocean: a review. J. Sea Res. 53 (1), 25–42.
Shchepetkin, A.F., McWilliams, J.C., 2005. The regional oceanic modeling system (ROMS): a split-explicit, free-surface, topography-following-coordinate oceanic model. Ocean Model 9 (4), 347–404.
Shchepetkin, A.F., McWilliams, J.C., 2009. Correction and commentary for "Ocean forecasting in terrain-following coordinates: formulation and skill assessment of the regional ocean modeling system" by Haidvogel et al., J. Comp. Phys., 227, 3595–3624. J. Comput. Phys. 228 (24), 8985–9000.
Shelley, R.U., et al., 2012. Controls on dissolved cobalt in surface waters of the Sargasso Sea: comparisons with iron and aluminum. Glob. Biogeochem. Cycles 26 (2), GB2020. https://doi.org/10.1029/2011GB004155.
Slawyk, G., Collos, Y., Auclair, J.C., 1977. The use of the ^{13}C and ^{15}N isotopes for the simultaneous measurement of carbon and nitrogen turnover rates in marine phytoplankton. Limnol. Oceanogr. 22, 925–932.
Taguchi, S., Jones, D., Hirata, J.A., Laws, E.A., 1987. Potential effect of ocean thermal energy conversion (OTEC) mixed water on natural phytoplankton assemblages in Hawaiian waters. Bull. Plankton Soc. JapanJapan 34 (2), 125–142.
Teira, E., Mouriño, B., Marañón, E., Pérez, V., Pazó, M.J., Serret, P., de Armas, D., Escánez, J., Woodward, E.M.S., Fernández, E., 2005. Variability of chlorophyll and primary production in the Eastern North Atlantic Subtropical Gyre: potential factors affecting phytoplankton activity. Deep Sea Res., Part I 52 569–288.
Thomas, C.R., 1996. Identifying Marine Phytoplankton. Academic Press, Inc. San Diego, California.
Tovar-Sanchez, A., Sañudo-Wilhelmy, S.A., 2011. Influence of the Amazon River on dissolved and intra-cellular metal concentrations in *Trichodesmium* colonies along the western boundary of the sub-tropical North Atlantic Ocean. Biogeosciences 8, 217–225.
Uitz, J., Claustre, H., Gentili, B., Stramski, D., 2010. Phytoplankton class-specific primary production in the world's oceans: seasonal and interannual variability from satellite observations. Glob. Biogeochem. Cycles 24 (3).
Van Oostende, N., Dunne, J.P., Fawcett, S.E., Ward, B.B., 2015. Phytoplankton succession explains size-partitioning of new production following upwelling-induced blooms. J. Mar. Syst. 148, 14–25.
WoRMS Editorial Board, 2019. World Register of Marine Species.Available from. http://www.marinespecies.orgatVLIZ Accessed 2019-06-21. https://doi.org/10.14284/170.